Spectroscopic Characterization of Doped Poly(benzidine) and Its Nanocomposite with Cationic Clay

Gustavo M. do Nascimento, Vera R. L. Constantino, and Marcia L. A. Temperini*

Departamento de Química Fundamental, Instituto de Química, Universidade de São Paulo, CP 26.077, CEP 05513-970, São Paulo, SP, Brazil

Received: October 29, 2003; In Final Form: February 17, 2004

The resonance Raman spectroscopic characterization of doped poly(benzidine) and poly(benzidine)−clay nanocomposites is reported for the first time. The montmorillonite clay was used as a host structure to confine the polymer. The organic−inorganic hybrid materials were synthesized by oxidative polymerization of benzidinium ions intercalated in the host's nanospace. The formation of poly(benzidine) between the layers was confirmed by X-ray diffraction and scanning electron microscopy. The correlation between the Raman bands in the spectra of the free doped poly(benzidine) and those of the intercalated polymers indicates that the chain structures of free and intercalated polymers have the same chromophoric segments. The resonance Raman spectra of free and intercalated poly(benzidine) polymers show bands at 1140 and 1445 cm^{-1} which indicate the presence of N═N bonding in the polymeric chains and also weak bands at 1400 and 1414 cm^{-1} indicating that phenazine-like segments are formed in a lesser extension. The results are also confirmed by X-ray absorption spectroscopy at the N K-edge. The electrical conductivity of poly(benzidine)−clay nanocomposites is about 10^{-4} $S{\cdot}cm^{-1}$, which is of the same magnitude as that observed for free doped poly(benzidine). The EPR spectra of the nanocomposites show a low intensity signal.

Introduction

The interest in the synthesis and characterization of polymer−clay nanocomposites has increased in recent years, as such new materials often exhibit physical properties superior to those of the macroscale composites, making their technological application attractive. The main purpose for performing the polymer confinement in porous frameworks, such as clays, is to work at the molecular level in order to create specific supramolecular arrangements of its chains with a possible improvement of the polymer bulk properties.[1] The polymer−clay nanocomposites can show electronic, mechanical, magnetic, and optical properties that are not present or are not significant in the individual phases.

The structure of clay minerals of the smectite group consists of a central sheet of $MO_4(OH)_2$ octahedra symmetrically bound to two MO_4 tetrahedral sheets producing layers designated T:O:T. The octahedral sites are occupied by ions such as aluminum, magnesium, and iron, while the tetrahedral centers accommodate silicon and aluminum. The negative T:O:T individual layers assume a parallel orientation, and the electric charge is neutralized by the presence of exchangeable hydrated positive ions in the interlayer space.[2] These layered crystalline silicates show great capacity for surface adsorption and also catalytic activity in organic reactions. Montmorillonite (MMT) is the most common smectite clay, with its negative layer charge arising mainly from the substitution of octahedral aluminum by magnesium (II) ions.

Several polymers have been synthesized in the nanospace of the clay interlayers, such as poly(ethylene oxide),[3] poly(styrene),[4] and conducting polymers such as poly(aniline),[5,6] poly(pyrrole),[7] poly(*o*-methoxyaniline),[8] and poly(2-ethynylpyridine).[9] The major interest in the synthesis of novel conducting polymer−clay nanocomposites lies in the possibility of enhancing the conductivity and electrochromic activity of the bulk polymer. Although significant progress has been made in developing nanocomposites, until now it has been very difficult to predict and control their properties.[10]

Our interest is to carry out the vibrational and electronic characterization of conducting polymers intercalated in layered materials such as clays, in order to give subsidies for the understanding of the structure−property relationships in these nanocomposites. Raman spectroscopy has been extremely useful in the structural characterization of conjugated polymers.[11] In fact, by means of the resonance Raman effect it is possible to identify the bands of each chromophoric species in the polymeric chains, thus providing unique information about vibrational frequencies and electronic transitions. It is this property, chromophore selectivity, that makes the resonance Raman technique so attractive for the study of conducting polymers. In our previous work[12] using resonance Raman spectroscopy for characterizing poly(aniline)−MMT, it was shown that polymerization of intercalated anilinium leads to poly(aniline) having tail to tail (benzidine) and head to tail (*p*-phenylenediamine) segments. It must be emphasized that with the use of only vibrational IR spectroscopy it is not possible to get this information because of the low signal/noise ratio of the polymer bands and the predominance of the layered silicate bands in the spectrum.

To our knowledge no work has yet been published on the synthesis of poly(benzidine) (PBZ) in confined environments. The electrochemical and chemical syntheses of PBZ in solution have been reported in the literature,[13−15] but some doubts concerning the structure of the polymeric chains still remain.

It is well documented that colorless aromatic amines such as benzidine (BZ), 4,4′-diamine-biphenyl, form colored species in contact with clay minerals.[16−18] The BZ is oxidized to its blue monovalent semiquinone radical cation ($BZ^{+\bullet}$; absorption

10.1021/jp037262i CCC: $27.50
Published on Web 04/07/2004

maximum at ca. 580 nm) and also to the yellow divalent quinone (BZ^{2+}; absorption maximum at ca. 444 nm). In acidic solutions (pH < 2), the yellow species is dominant, and at pH > 4.2, the blue species prevails. It is suggested that atmospheric molecular oxygen and/or the Fe^{3+} ions in the octahedral center of the clay sheet are the electron acceptors.[18] It was also noticed that the wet blue BZ−clay samples become yellow after drying.

The assignment of the vibrational spectra of BZ and its oxidized species can be found in the literature[19,20] as well as the attribution for the BZ−clay systems.[21] In a characterization study of poly(diphenylamine), PDPA, a polymer with a PBZ-like structure, the frequencies of the Raman and IR bands of neutral, radical cation, and dication of benzidine segments in the polymeric chains have been determined.[22,23] With the use of the resonance Raman technique, it was shown that during PDPA thermal treatment, new oxidized structures, having the oxazine chromophoric rings, were formed.[24] The data obtained in these studies are used in the present work to characterize the free PBZ and PBZ−MMT nanocomposites.

The aims of the present work are the intercalation and polymerization of benzidinium ions into the smectite clay montmorillonite (MMT) at two different pH values, as well as the textural and spectroscopic characterizations of the poly(benzidine)−montmorillonite (PBZ−MMT) nanocomposites. To reach such goals, X-ray diffraction (XRD), scanning electron microscopy (SEM), FTIR absorption, resonance Raman, electronic paramagnetic resonance (EPR), and X-ray absorption near edge (XANES) spectroscopies were employed. The data obtained for PBZ−MMT nanocomposites are compared to those of free doped PBZ and poly(aniline)−MMT, in order to understand the role of the confined environment in the structure of the polymeric chain.

Experimental Section

Preparation of Doped Poly(benzidine) (PBZ−HCl). PBZ was synthesized from an adapted procedure from ref 13. Benzidine (BZ) was obtained by deprotonation of 0.5 g of benzidine dichloride (H_2BZCl_2) (Sigma) by its reaction with 20 mL of an aqueous solution of 1 mol/L NaOH (Merck) while being stirred at room temperature for 2 days. The precipitated white solid was isolated by filtration and dried by dynamic vacuum. The formation of neutral BZ was confirmed by elemental analysis. The following data were found. Analysis calculated for $C_{12}H_{12}N_2$: C, 78.2%; H, 6.56%; N, 15.2%. Found: C, 78.0%; H, 6.86%; N, 15.3%. The polymerization of BZ was carried out using the same amount of BZ/persulfate as that reported in the literature.[13] A total of 5.5 mL of acetonitrile (Aldrich) solution containing 0.1 g of BZ was maintained in an ice−water bath while 0.2 mL of aqueous solution containing 0.02 g of ammonium persulfate (Merck) was slowly added dropwise. The mixture was stirred in the ice−water bath for 12 h. The blue solid that formed, assigned as neutral PBZ, was isolated by filtration and dried under dynamic vacuum. The doped PBZ−HCl was synthesized by adding 0.05 g of neutral PBZ in 10 mL of an aqueous solution of 1mol/L HCl (Merck). The mixture was stirred continuously at room temperature for 1 day. A brown solid was isolated by filtration, and it was dried under vacuum. The UV−vis−NIR spectrum shows a broad absorption band from 250 to 800 nm with maximum in the 300−500 nm range.

Preparation of PBZ−MMT Clay Nanocomposite. SWy2 montmorillonite clay (MMT) from the Clay Minerals Repository was treated with sodium chloride and size fractionated to obtain the homoionic Na^+ form, free of main impurities. The following experimental procedure was adapted from the method previously used by us for the intercalation of aniline into MMT clay.[12] A total of 40 mL of an aqueous suspension containing 1 g of MMT was slowly dropped into 60 mL of a stirred aqueous solution containing 0.02 mol/L of BZ dichloride and 0.04 mol/L of HCl at room temperature. As soon as the reagents were mixed, the solid particles became blue, the characteristic color of benzidine radical cation ($BZ^{+\bullet}$). After some hours the color changed to violet. After stirring for 12 h at room temperature, the suspension was filtered (filter Millipore 0.22 μm) and the H_2BZ^{2+}−MMT was washed with deionized water until the excess benzidinium (H_2BZ^{2+}) was eliminated. Then, the H_2BZ^{2+}−MMT material was dried under dynamic vacuum and kept in a desiccator. For the polymerization of the intercalated benzidinium ions, 1 g of H_2BZ^{2+}−MMT was suspended in 100 mL of stirred deionized water for 30 min. The suspension was divided into two fractions. For one of them, the pH was adjusted to about 2 by the addition of 1mol/L of an aqueous HCl solution while for the other, the pH was not adjusted (the pH of the suspension was ca. 5). Afterward 0.0445 g of ammonium persulfate was added to each fraction, and the suspensions were stirred for 24 h at room temperature. The suspensions were filtered (filter Millipore 0.22 μm), and the isolated brown solids (abbreviated PBZ−MMT) were dried under dynamic vacuum and stored in a desiccator. The UV−vis−NIR spectra of the two solid samples show a broad absorption band from 220 to 1300 nm with maximum in the 600−900 nm range.

Instrumentation. Resonance Raman spectra using the 632.8 nm exciting radiation (He−Ne laser, Spectra Physics, model 127) and the 457.9, 488.0, and 514.5 nm exciting radiations (Ar^+ laser, Omnichrome model 543-AP) were recorded with a Renishaw Raman imaging microscope (System 3000) containing a Olympus metallurgical microscope and a CCD detector (cooled by a Peltier). The laser beam was focused on the sample in a roughly 1 μm spot by a ×80 lens. The laser power was always kept below 0.7 mW at the sample to avoid sample degradation. FT-Raman spectra of solid samples were recorded in an RFS 100 FT-Raman Bruker spectrometer with the 1064 nm radiation from a Nd:YAG laser. The FTIR spectra were obtained using a BOMEM MB-100 instrument with a resolution of 4 cm^{-1}, and the samples were dispersed in KBr pellets.

Diffuse reflectance spectra of solids dispersed in $BaSO_4$ were recorded in a Shimadzu UVPC-3101 scanning spectrophotometer, using an integration sphere attachment.

XRD patterns of oriented films were obtained in a Phillips MPD-1880 diffractometer using Cu Kα radiation. EPR spectra of solid samples were recorded at room temperature on a Bruker ER 200 spectrometer operating in the X-band (∼9.5 GHz).

The material resistivities were measured by the two-points method using an Autolab PGSTAT30 impedance analyzer (Ecochemie) with an FRA module. A dc potential of 0.0 V with a modulation of 5 mV (rms) was imposed in the 10 kHz to 10 MHz frequency range.

XANES spectra were obtained using the facilities of the National Synchrotron Light Laboratory (LNLS), Brazil. The SGM beam line has a focused beam of roughly a 0.5 mm^2 spot, and the spectra were recorded in total electron yield detection with the sample compartment pressure at 10^{-8} mbar. All energy values in the N K-edge spectra were calibrated using the first resonant peak in the N K-edge XANES spectrum of potassium nitrate.[25]

SEM images of the samples, recovered by 16 nm of sputtered gold film, were recorded through a low vacuum scanning

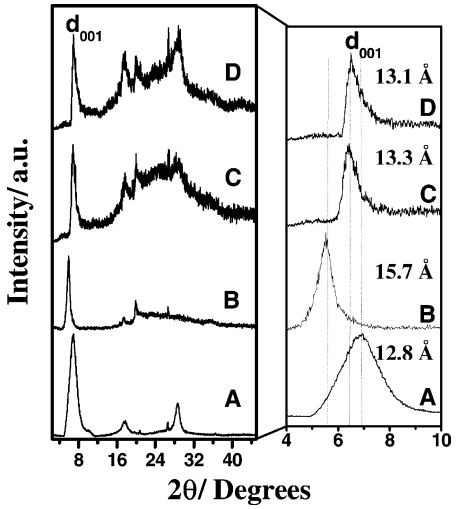

Figure 1. X-ray diffraction patterns of powder samples: (A) Na^+-MMT; (B) H_2BZ^{2+}−MMT; (C) PBZ−MMT prepared at pH 5; (D) PBZ−MMT prepared at pH 2.

electron microscope (SEM, JSM-5900LV) operated with a high-tension voltage of 10 kV.

Results and Discussion

Figure 1 shows the XRD patterns of MMT samples (the Na^+ form and the H_2BZ^{2+} intercalated forms before and after the polymerization reaction). The sodium substitution by H_2BZ^{2+} ions in the interlayer region causes an increase in the MMT basal spacing from 12.8 Å to 15.7 Å, a result similar to that observed in previous work.[17] These data suggest that H_2BZ^{2+} is intercalated in a tilt orientation relative to the layer and/or in a parallel disposition in an interlayer region containing a water bilayer. Besides H_2BZ^{2+}, the interlayer should accommodate the oxidized blue species $BZ^{+\bullet}$ and, maybe, in minor amount, the BZ^{2+} species (see Scheme 1). It has been claimed that the aromatic ring flat orientation is responsible for the blue

SCHEME 1: Schematic Representation of the Intercalation and Polymerization Processes of BZ in MMT

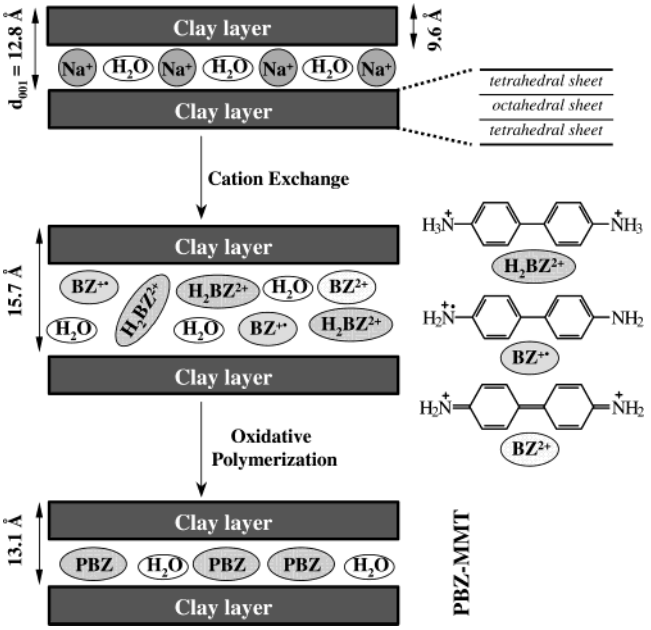

benzidine radical cation ($BZ^{+\bullet}$) stabilization in the clay environment.[18] After the H_2BZ^{2+} polymerization between the clay layers, the basal spacing decreases to 13.3 Å and 13.1 Å for the samples prepared at pH 5 and pH 2, respectively. Figure 1 also shows that the layer stackings of PBZ−MMT composites are less organized in the *c* axes when compared to the precursor containing the monomer. A basal spacing of about 13 Å for PBZ−MMT nanocomposites suggests that the intercalated polymeric chains lie flat between the layers (see Scheme 1). Similar data were found for the intercalated poly(aniline) in MMT.[12] In order to get information about the polymeric chains structure of the intercalated PBZ, spectroscopic characterization was performed, and the results will be shown later.

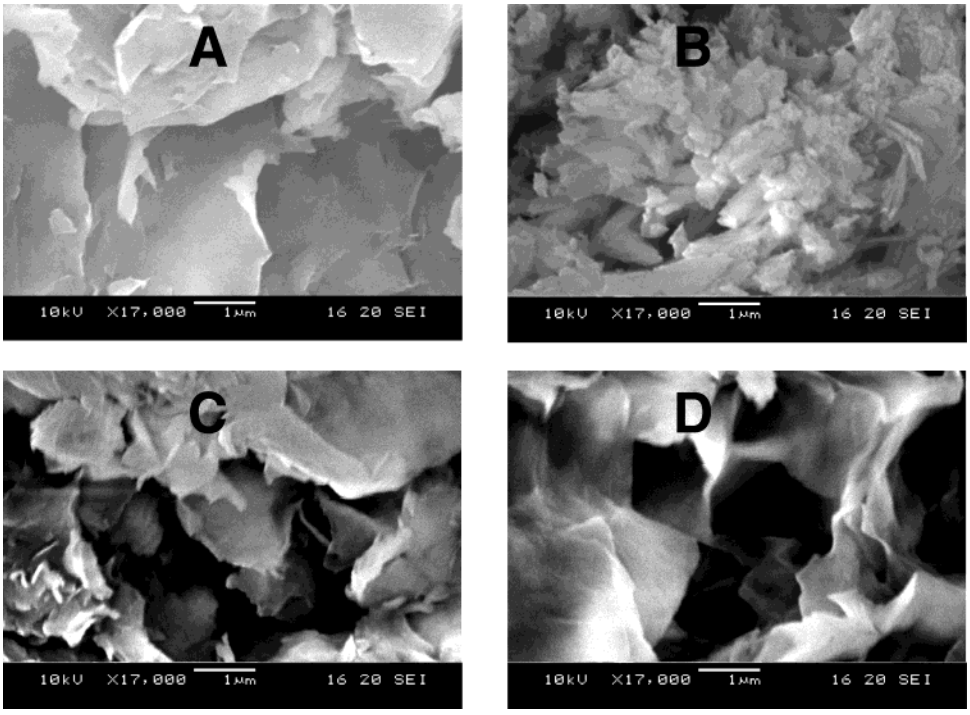

Figure 2. SEM images of (A) Na^+-MMT, (B) undoped PBZ, (C) PBZ−MMT prepared at pH 5, and (D) PBZ−MMT prepared at pH 2.

SCHEME 2: Schematic Representation of Probable Chromophoric Segments Present in the PBZ Chains

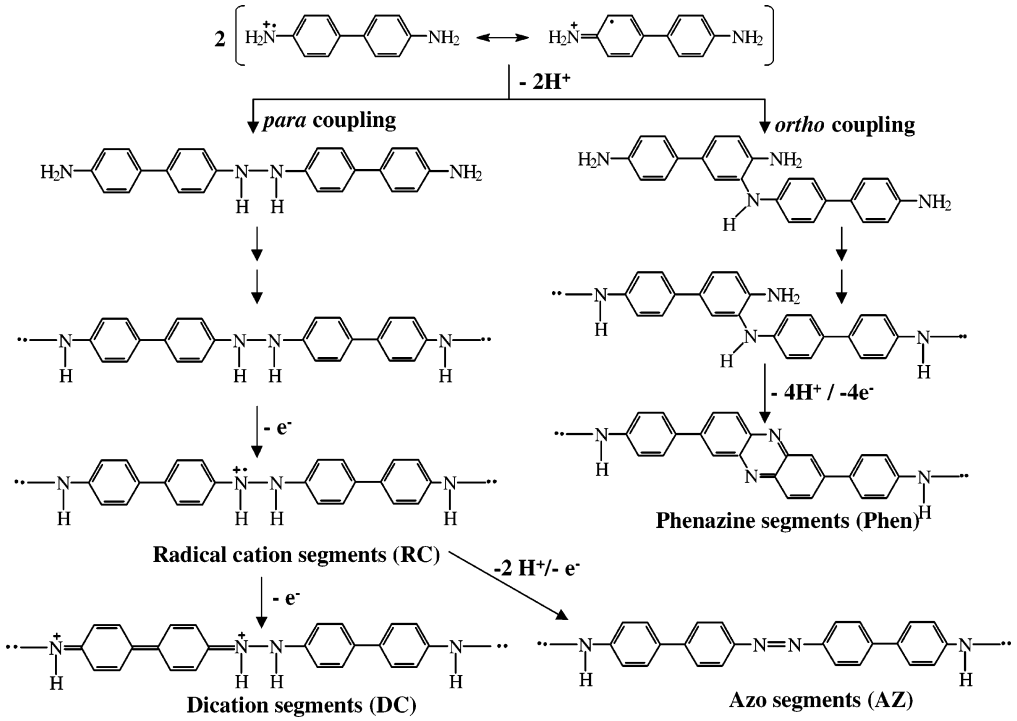

The morphological aspects of PBZ−MMT nanocomposites were investigated by scanning electron microscopy (SEM) (see Figure 2). It is possible to notice that the morphologies of the PBZ−MMT nanocomposites (images C and D) are similar to that of the Na^+-MMT (image A) but very different from that of free undoped PBZ (image B), showing that the polymerization occurs mainly between the clay layers thus corroborating the XRD data. Another important characteristic of the PBZ−MMT SEM images is the homogeneous aspect of the nanocomposite samples, indicating the absence of domains.[26]

During the BZ oxidative polymerization, the $BZ^{+\bullet}$ species can undergo para (N−N) or ortho (N−C) coupling reactions giving linear PBZ chains, as can be seen in Scheme 2. It is also possible that after the N−C coupling, some cyclization occurs. These kinds of reactions as well as oxidation and deprotonation can generate chromophoric segments, such as hidrazo, radical cation, dication, phenazine, and azo, in the polymeric chains (see Scheme 2). Thus the resonance Raman analysis was conducted considering such possibilities.

Figure 3 shows the resonance Raman spectra of free doped PBZ for different excitation wavelengths, and Table 1 presents a tentative assignment for the bands in the 1100−1800 cm^{-1} region. The bands at 1140, 1445, and 1498 cm^{-1}, with high relative intensities at 488 nm, are observed in the spectrum of *trans*-azobenzene (Figure 4A) at 1146 (ν_{C-N} stretching), 1440 ($\nu_{N=N}$ stretching), and 1491 cm^{-1} (ν_{C-C} stretching), respectively.[27] The presence of these bands in the spectra of the polymer indicates that para coupling reactions are occurring during the polymerization. When 632.8 nm is used as the exciting radiation, there is an increase in the relative intensities of the bands at 1286, 1310, and 1350 cm^{-1}. These bands can be attributed to the inter-rings ν_{C-C} stretching of the azo, radical cation, and dication segments, respectively, in the polymeric chains[23,24] (see Scheme 2). The variations in the frequency values for these species are due to the degree of the double bond character of the inter-rings C−C of the diphenyl moiety.

D'Eramo et al.[15] have studied the electrochemical polymerization of benzidine, and the PBZ formed was characterized by the FTIR technique. It was proposed that the ortho (N−C) coupling reaction, giving linear polymeric chains, is more favored than the para (N−N) coupling reaction in the electrochemically formed PBZ. The resonance Raman results presented here indicate that N−N coupling is occurring at a significant extension during the chemical polymerization. The authors also argued that the presence of some IR bands suggests that, after the N−C coupling, cyclization occurs giving phenazine-like segments in the polymeric chain. In order to clarify this point, Figure 4B shows the FT-Raman spectrum of phenazine. Its most intense bands at 1403 cm^{-1} (ν_{C-C} phen ring) and a shoulder at 1417 cm^{-1} (combination band)[28,29] could be related to the weak bands at 1400 and 1414 cm^{-1} in the spectra of free doped PBZ at 514.5 and 488.0 nm excitation wavelengths (Figure 3). These data suggest that in the synthetic route used in this work, phenazine rings are also formed in the polymeric chains. If one assumes that the resonance enhancement factors for the azo and phenazine chromophoric segments at the 488.0 nm wavelength

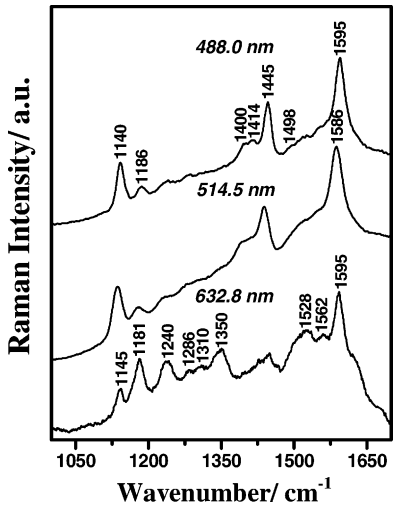

Figure 3. Resonance Raman spectra of powder samples of free doped PBZ obtained at 632.8, 514.5, and 488.0 nm excitation wavelengths.

TABLE 1: Experimental Frequency Values, Relative Intensities, and Tentative Assignment of the Raman Bands of Doped PBZ and PBZ−MMT Prepared at pH 5[a]

632.8 nm		514.5 nm		488.0 nm		tentative
PBZ	PBZ−MMT	PBZ	PBZ−MMT	PBZ	PBZ−MMT	assignment
	1140 *sh*	1140 *ms*	1144 *w*	1140 *ms*	1144 *ms*	ν_{C-N} AZ
1145 *m*[b]	1165 *ms*					β_{C-H} DC
1181 *ms*	1188 *sh*	1181 *w*	1188 *w*			β_{C-H} RC
				1186 *w*	1207 v*w*	β_{C-H} AZ
1240 *ms*	1245 *w*	1240 *w*	1245 *w*	1240 *w*	1245 *w*	
1286 *w*	1280 *w*		1280 *w*		1280 *w*	$\nu_{C-C\ inter-ring}$ AZ
1310 *w*		1310 *w*	1305 *w*		1305 *vw*	$\nu_{C-C\ inter-ring}$ RC
1350 *ms*	1365 *s*		1365 *m*		1365 *w*	$\nu_{C-C\ inter-ring}$ DC
		1400 *m*		1400 *m*		ν_{C-C} phen
1414 *w*		1414 *m*	1408 *m*	1414 *m*	1408 *m*	ν_{C-C} phen
1445 *m*	1445 *vw*	1445 *ms*	1445 *ms*	1445 *ms*	1445 *ms*	$\nu_{N=N}$ AZ
		1505 *w*	1505 *w*	1498 *w*	1505 *w*	ν_{C-C} AZ
1528 *w*	1535 *w*	1530 *w*	1535 *w*			ν_{C-N} DC
1562 *w*	1575 *sh*		1570 *s*		1575 *sh*	ν_{C-C} RC
		1586 *s*[c]			1596 *s*	ν_{C-C} AZ
1595 *s*	1596 *s*		1596 *s*	1595 *s*		ν_{C-C} DC

[a] The symbols AZ, RC, and DC represent the azo, radical cation, and dication segments respectively. [b] *s* = strong, *ms* = medium strong, *m* = medium, *w* = weak, *vw* = very weak, *sh* = shoulder. [c] Unresolved bands.

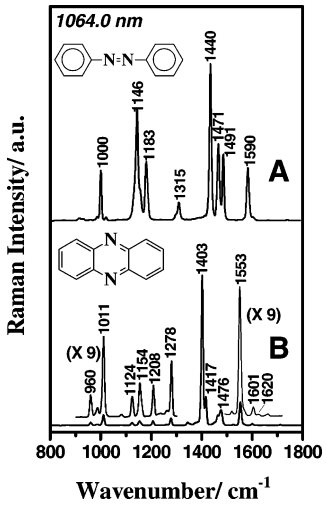

Figure 4. FT-Raman spectra of (A) solid azobenzene and (B) solid phenazine.

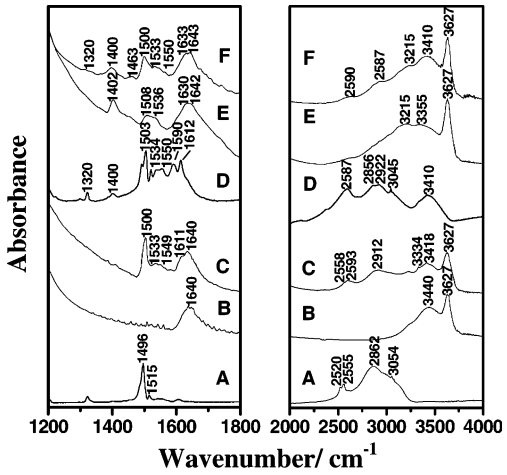

Figure 5. FTIR spectra of (A) H_2BZCl_2, (B) Na^+-MMT, (C) H_2BZ^{2+}−MMT, (D) doped PBZ, (E) PBZ−MMT prepared at pH 2, and (F) PBZ−MMT prepared at pH 5.

are the same, the high relative intensities of the azo bands compared to the phenazine bands indicate that the para coupling reactions are favored in the chemical polymerization of doped PBZ. XANES data of free doped PBZ discussed later confirm this statement. Summarizing, these results indicate that azo bonds (resonance Raman condition at blue excitation wavelengths), radical cation and dication units (resonance condition at red wavelengths), and phenazine-like segments are presented in the free doped PBZ chains (see Scheme 2).

Figure 5 shows the IR spectra of Na^+-MMT, the free and confined monomer, and polymers. The FTIR technique has been extensively used for characterizing benzidine−clay systems.[18] In the H_2BZ^{2+} spectrum (Figure 5A) the bands at 1496, 2862, and 3054 cm^{-1} can be assigned respectively to the ν_{C-C} ring, ν_{NH3+}, and ν_{C-H} ring of the monomer.[30] In the spectrum of Na^+-MMT (Figure 5B) the bands at 1640 and 3440 cm^{-1} have been assigned to bending and stretching modes of adsorbed water, respectively, while the band at 3627 cm^{-1} has been attributed to the ν_{O-H} stretching of structural hydroxyl groups.[31] All the bands of the monomer and the layered silicate are observed in the spectrum of H_2BZ^{2+}−MMT (Figure 5C), while weak bands at circa 1549 and 1611 cm^{-1} could be due to the dication BZ^{2+}.[30] The FTIR spectra of PBZ−MMT prepared at two different pH values are very similar (parts E and F of Figure 5), and the new bands at 1320 and 1400 cm^{-1}, also observed in the spectrum of free doped PBZ (Figure 5D), confirm the formation of intercalated PBZ, thus corroborating the XRD data. However, it is difficult to characterize the majority of the segments present in the polymeric chain of intercalated PBZ by the FTIR technique (the spectra of PBZ−MMT samples are dominated by the clay's bands). So, resonance Raman spectroscopy was used to better characterize the nanocomposites.

Figure 6 shows the resonance Raman spectra of PBZ−MMT nanocomposites prepared at pH 2 and pH 5 for the excitation wavelengths indicated. When these spectra are compared to those of the free doped PBZ (Figure 3), the first point that must be emphasized is the correlation between the frequencies of the bands in the spectra (see Table 1), indicating that the same kind of coupling reactions are occurring in the interlayer polymerization. There are shifts in the frequencies of some bands of the intercalated PBZ that can be accounted for by the interaction with the layered silicate. Once again the Raman bands that can be assigned to phenazine moieties show very low intensities, indicating that ortho (N−C) coupling followed by cyclization is not the preferential polymerization route inside the clay. This conclusion will be confirmed by the XANES data.

As was observed in the Raman spectra of free doped PBZ, in the spectra of intercalated PBZ the resonance Raman

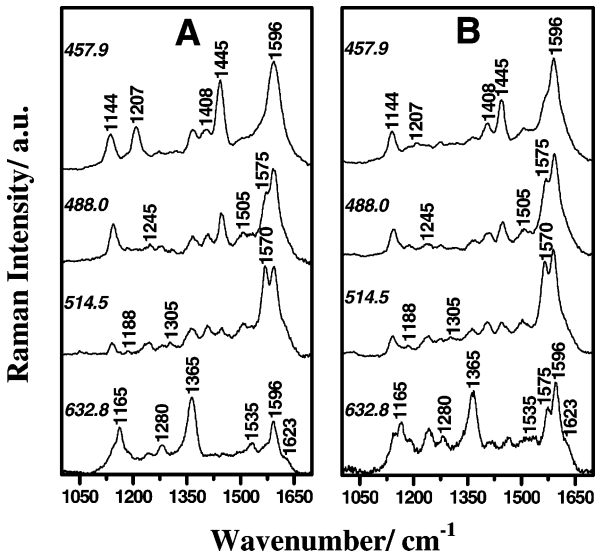

Figure 6. Resonance Raman spectra of powder samples: (A) PBZ−MMT prepared at pH 5 and (B) PBZ−MMT prepared at pH 2, at the indicated excitation wavelengths.

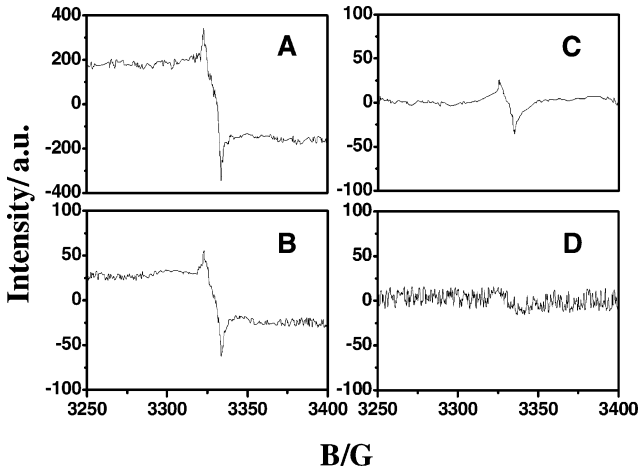

Figure 7. EPR spectra of powder samples: (A) PBZ−MMT prepared at pH 2; (B) PBZ−MMT prepared at pH 5; (C) H_2BZ^{2+}−MMT; (D) Na^+-MMT.

conditions for the azo, radical cation, and dication chromophoric units present in the PBZ−MMT chains are different. So, for the 457.9 nm excitation line, there is an increase in the relative intensities of the bands at 1144 and 1445 cm^{-1} assigned to the azo segments, while for the 632.8 nm excitation radiation, the bands at 1165, 1365, and 1596 cm^{-1}, attributed to dication segments, are enhanced. When 514.5 nm is used as the excitation wavelength, the bands at 1188, 1305, and 1570 cm^{-1}, assigned to the radical cation, are observed in the spectra.

If we consider the same excitation wavelength, the difference in the relative intensities of the bands in the spectra of free (Figure 3) and confined PBZ (Figure 6) can be assigned to the relative amounts of the segments in the polymeric chains. For instance, choosing the spectra at 488.0 nm exciting radiation, the relative intensities of the bands at circa 1144 and 1445 cm^{-1} in the spectra of the confined polymers and in the free polymer are quite similar, indicating that the amount of N═N azo bonds are almost the same in the free and confined PBZ chains. Nevertheless, a closer inspection of the spectra of the nanocomposites shows that the relative intensities of the bands at 1144 and 1445 cm^{-1} in the spectrum of the confined polymer prepared at pH 5 are higher than in the spectrum of the one prepared at pH 2, indicating that there are more azo bonds in the polymeric chains of the former. The presence of more azo units in the spectrum of the PBZ−MMT prepared at pH 5 is also confirmed by an increase of the band at 1207 cm^{-1}, assigned to β_{C-H} of the aromatic ring. This result is in agreement with the proposed reactions in Scheme 2: low-pH solutions do not favor the azo bond formation.

Considering the 632.8 nm excitation radiation, the high relative intensities of the bands at 1165, 1365, and 1596 cm^{-1}, attributed to the dication units in the spectra of the confined polymers, indicate that there are more dication segments than radical cation units. The observation of the bands at 1188 and 1575 cm^{-1}, attributed to the radical cation, in the spectrum of PBZ−MMT prepared at pH 2 suggests that the acidic medium favors the formation of the radical cation.

These results are confirmed by EPR measurements (Figure 7). The spectrum of the confined polymer prepared at pH 2 (Figure 7A) presents a very low signal but higher than that observed in the spectrum of the confined polymer prepared at pH 5 (Figure 7B). In this figure is also presented the EPR spectrum of H_2BZ^{2+}−MMT (Figure 7C), where a weak signal was observed, confirming the presence of the semiquinone radical cation, $BZ^{\bullet+}$, which corroborates the FTIR data (Figure 5C). No EPR signal was observed in the spectrum of Na^+-MMT (Figure 7D).

The conductivity values are 2×10^{-4} S·cm^{-1} for PBZ−MMT prepared at pH 2 and 1×10^{-4} S·cm^{-1} for the nanocomposite prepared at pH 5. Kumar et al.[13] reported the values of about 10^{-7} and 10^{-4} S·cm^{-1} for the electrical conductivity of undoped and doped PBZ−H_2SO_4, respectively. Considering that the nanocomposites are also formed by the MMT (an insulator), the same magnitude of the conductivity values obtained for free and intercalated PBZ means that there is an enhancement in the electrical conductivity of the confined polymeric chains. We have also observed the same conductivity values for secondarily doped poly(diphenylamine) (ca. 10^{-4} S·cm^{-1}) where the dications are the free charge carriers.[24] Taking into account that both PBZ−MMT samples show a predominant diamagnetic behavior, one can suggest that the dication units are responsible for the nanocomposite's electrical conductivity.

X-ray absorption near the nitrogen K-edge structure (N K XANES), that promotes electron core excitation, is an excellent technique for distinguishing different types of nitrogen compounds.[32,33] Henning et al.[34] demonstrated the viability of using the XANES technique to characterize the different oxidation states of nitrogen atoms in the poly(aniline), PANI, chain. In the N K XANES spectrum of the emeraldine salt form of PANI (PANI-ES), the peaks at 397.4, 398.8, and 402.1 eV were assigned to N1s → 2pπ* of imine, protonated imine, and amine nitrogens, respectively. In the present work, the XANES technique has been used for identifying the nature of the nitrogen atoms in the PBZ chains. For the assignment of the peaks in the XANES spectra of PBZ polymers, some compounds were used as standard compounds, such as Congo red (having amine nitrogen and azo bonds), phenazine (imine nitrogen ring), Nile blue (having amine, positive imine nitrogen, and imine nitrogen ring) and PANI-ES (see structures in Table 2). As is known, the absorption peaks at the low-energy region can be attributed to N1s → 2pπ* (see Table 2), while the peaks at higher energies are related to the N1s → s* transition.[33]

The XANES spectra of PBZ−MMT nanocomposites are similar (parts F an G of Figure 8), confirming the same kind of intercalated polymeric chains. In the spectrum of free doped PBZ (Figure 8E) the band at 398.7 eV is the strongest in the spectrum. This band can be assigned to azo nitrogens, once it

TABLE 2: N1s → 2pπ* Resonances Energies Observed for Standard Compounds

Compound	Structural Formula	Resonance Energy/ eV N1s →π*					
		=N- Phenazinic or Oxazinic ring	-N=N-	$-\overset{+\bullet}{N}=$	$-\overset{+}{N}=$	=N-	-NH-
Congo Red	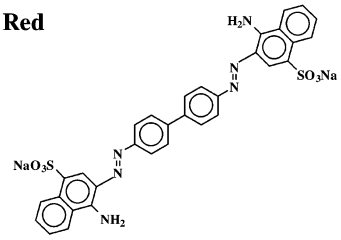		398.7				402.5
Phenazine	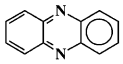	398.2				400.6	
Nile blue	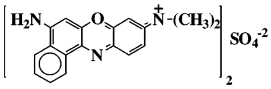	398.3			399.6		
PANI-ES				399.1			402.7

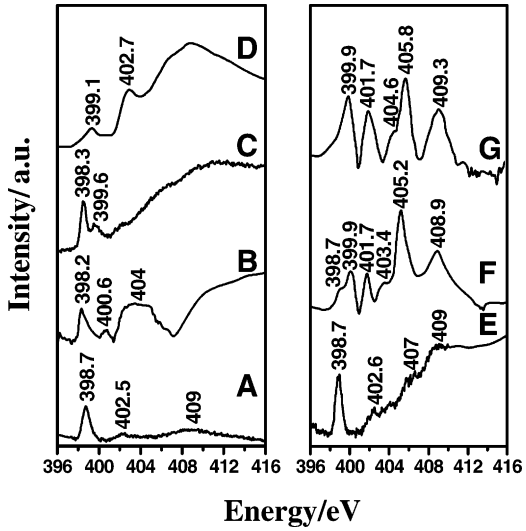

Figure 8. XANES spectra in the N K-edge of (A) Congo red azo dye, (B) phenazine, (C) Nile blue, (D) PANI-ES, (E) doped PBZ, (F) PBZ−MMT prepared at pH 5, and (G) PBZ−MMT prepared at pH 2.

was observed in the spectrum of Congo red (Figure 8A). On the other hand, the azo band has low relative intensity in the spectrum of PBZ−MMT prepared at pH 5 (Figure 8F) and it appears as a shoulder in the PBZ−MMT prepared at pH 2 (Figure 8 G). These results reinforce the presence of azo bonds in free and intercalated PBZ. The band at 399.9 eV observed in the spectra of confined polymers is close to the band at 399.6 eV of Nile blue that corresponds to positive imine nitrogen. Also considering the Raman and EPR results of the confined polymers, which show that dication segments prevail over the radical cation, we are assigning the band at 399.9 eV to the dication segments in the polymeric chain (see Scheme 2). Another important observation is that the band of imine nitrogens of the phenazine ring at 398.2 eV (Figure 8B) is practically not seen in the spectra of the free and confined PBZ polymers, confirming the low amount of phenazine-like units in the chains. This result is in agreement with the Raman data. The tentative assignments of the other peaks in the spectra of the standard compounds are presented in Table 2.

The observation of the band at 1445 cm^{-1}, assigned to νN=N stretching, and its resonance Raman behavior in the spectra of free and intercalated PBZ confirm the previous assignment for this band in the spectrum of PANI−MMT[12] and reinforce the statement that during the polymerization of intercalated anilinium a head to head (N−N) coupling reaction also occurs.

Conclusions

The XRD and SEM data confirm that PBZ is formed between the clay layers. The basal spacing of about 13 Å observed in the XRD patterns of PBZ−MMT nanocomposites suggests that the intercalated polymer chains lie flat between the layers. The correlation between the frequencies of the bands in the resonance Raman spectra of free and intercalated PBZ indicates that the same kind of coupling reactions are occurring in the synthetic routes used. From the Raman and XANES results it was possible to infer that para (N−N) coupling reactions are favored in the synthetic routes used to prepare free and confined PBZ. Only small phenazine features have been observed in the Raman and XANES spectra of free and confined PBZ. Considering the confined PBZ polymers, there are more azo bonds in the PBZ−MMT prepared at pH 5. The polymeric chains of the PBZ−MMT nanocomposites present more dication segments than radical cation units. Resonance Raman and EPR results indicate that PBZ−MMT prepared at pH 2 has a higher number of radical cation segments than the intercalated polymer prepared at pH 5.

Very similar values of conductivity have been obtained for PBZ−MMT prepared at pH 5 and pH 2. These values are of the same magnitude as that observed for free PBZ−H_2SO_4, which can suggest that the PBZ intercalation enhances the polymer's electrical conductivity.

Acknowledgment. This work was supported by FAPESP (Brazilian agency). Fellowships from FAPESP (G. M. do

Nascimento) and CNPq (M. L. A. Temperini and V. R. L. Constantino) are gratefully acknowledged. The authors thank the National Synchrotron Light Laboratory (LNLS/Brazil) for XANES N K-edge (SGM 1026, 1427, and 2169) measurements and the LME/LNLS for technical support during electron microscopy measurements. The authors are also grateful to Dr. A. M. C. Ferreira for the EPR spectra, Dr. S. I. C. de Torresi for the conductivity measurements, and Miss P. M. Dias for providing the Na^+-MMT suspension.

References and Notes

(1) Schmidt, D.; Shah, D.; Giannelis, E. P. *Curr. Opin. Solid State Mater. Sci.* **2002**, *6*, 205.
(2) Mott, C. J. B. *Catal. Today* **1988**, *2*, 199.
(3) Vaia, R. A.; Sauer, B. B.; Tse, O. K.; Giannelis, E. P. *J. Polym. Sci., Polym. Phys.* **1997**, *35*, 59.
(4) Kim, Y. K.; Choi, Y. S.; Wang, K. H.; Chung, I. *J. Chem. Mater.* **2002**, *14*, 4990.
(5) Giannelis, E. P.; Mehrotra, V. *Solid State Commun.* **1991**, *77*, 155.
(6) Zeng, Q. H.; Wang, D. Z.; Yu, A. B.; Lu, G. Q. *Nanotechnology* **2002**, *13*, 549.
(7) Kanatzidis, M. G.; Tonge, L. M.; Marks, T. J.; Marcy, H. O.; Kannewurf, C. R. *J. Am. Chem. Soc.* **1987**, *109*, 3797.
(8) Yeh, J.-M.; Chin, C.-P. *J. Appl. Polym. Sci.* **2003**, *88*, 1072.
(9) Liu, H.; Kim, D. W.; Blumstein, A.; Kumar, J.; Tripathy, S. K. *Chem. Mater.* **2001**, *13*, 2756.
(10) Vaia, R. A.; Giannelis, E. P. *MRS Bull.* **2001**, *26*, 394.
(11) Batchelder, D. N. In *Optical Techniques to Characterize Polymer Systems*; Brässler, H., Ed.; Elsevier: Amsterdam, 1987; p 393.
(12) Do Nascimento, G. M.; Constantino, V. R. L.; Temperini, M. L. A. *Macromolecules* **2002**, *35*, 7535.
(13) Kumar, M. N.; Nagabhooshanam, M.; Rao, M. A.; Rao, M. B. *Cryst. Res. Technol.* **2001**, *36*, 309.
(14) D'Eramo, F.; Silber, J. J.; Arévalo, A. H.; Sereno, L. E. *J. Electroanal. Chem.* **2000**, *494*, 60.
(15) D'Eramo, F.; Silber, J. J.; Arévalo, A. H.; Sereno, L. *J. Electroanal. Chem.* **1995**, *382*, 85.
(16) Matsunaga, Y. *Bull. Chem. Soc. Jpn.* **1972**, *45*, 770.
(17) Tennakoon, D. T. B.; Thomas, J. M.; Tricker, M. J. *J. Chem. Soc., Dalton Trans.* **1974**, *20*, 2207.
(18) Yariv, S. In *Organo-Clay Complexes and Interactions*; Yariv, S., Cross, H., Eds.; Marcel Dekker: New York, 2002; p 463.
(19) Akyüz, S.; Akalin, E. *J. Mol. Struct.* **2003**, *651*, 571.
(20) Hester, R. E.; Williams, K. P. J. *J. Chem. Soc., Faraday Trans. 2* **1981**, *77*, 541.
(21) Soma, Y.; Soma, M. *Clay Miner.* **1988**, *23*, 1.
(22) De Santana, H.; Temperini, M. L. A.; Rubim, J. C. *J. Electroanal. Chem.* **1993**, *356*, 145.
(23) De Santana, H.; Matos, J. R.; Temperini, M. L. A. *Polymer* **1998**, *30*, 315.
(24) Do Nascimento, G. M.; Pereira da Silva, J. E.; Córdoba de Torresi, S. I.; Temperini, M. L. A. *Macromolecules* **2002**, *35*, 121.
(25) Vinogradov, A. S.; Akimov, V. N. *Opt. Spectrosc.* **1998**, *85*, 53.
(26) Ke, Y.; Long, C.; Qi, Z. *J. Appl. Polym. Sci.* **1999**, *71*, 1139.
(27) Biswas, N.; Umapathy, S. *J. Phys. Chem. A* **1997**, *101*, 5555.
(28) Bandyopadhyay, I.; Manogaran, S. *J. Mol. Struct. (THEOCHEM)* **2000**, *507*, 217.
(29) Durnick, T. J.; Wait, S. C. *J. Mol. Spectrosc.* **1972**, *42*, 211.
(30) Lacher, M.; Lahav, N.; Yariv, S. *J. Therm. Anal.* **1993**, *40*, 41.
(31) Madejová, J.; Komadel, P. *Clays Clay Miner.* **2001**, *49*, 410.
(32) Francis, J. T.; Hitchcock, A. P. *J. Phys. Chem.* **1992**, *96*, 6598.
(33) Hennig, C.; Hallmeier, K. H.; Bach, A.; Bender, S.; Franke, R.; Hormes, J.; Szargan, R. *Spectrochim. Acta, Part A* **1996**, *52*, 1079.
(34) Hennig, C.; Hallmeier, K. H.; Szargan, R. *Synth. Met.* **1998**, *92*, 161.